

The CT Scanner Facility at Stellenbosch University: An open access X-ray computed tomography laboratory



Anton du Plessis^{a,b,*}, Stephan Gerhard le Roux^a, Anina Guelpa^a

^a CT Scanner Facility, Central Analytical Facilities, Stellenbosch University, Stellenbosch, South Africa

^b Physics Department, Stellenbosch University, Stellenbosch, South Africa

ARTICLE INFO

Article history:

Received 22 July 2016

Received in revised form 5 August 2016

Accepted 5 August 2016

Available online 23 August 2016

Keywords:

Industrial CT

X-ray tomography

Micro-computed tomography

Nano-computed tomography

3D imaging

Non-destructive testing

Non-destructive analysis

ABSTRACT

The Stellenbosch University CT Scanner Facility is an open access laboratory providing non-destructive X-ray computed tomography (CT) and a high performance image analysis services as part of the Central Analytical Facilities (CAF) of the university. Based in Stellenbosch, South Africa, this facility offers open access to the general user community, including local researchers, companies and also remote users (both local and international, via sample shipment and data transfer). The laboratory hosts two CT instruments, i.e. a micro-CT system, as well as a nano-CT system. A workstation-based Image Analysis Centre is equipped with numerous computers with data analysis software packages, which are to the disposal of the facility users, along with expert supervision, if required. All research disciplines are accommodated at the X-ray CT laboratory, provided that non-destructive analysis will be beneficial. During its first four years, the facility has accommodated more than 400 unique users (33 in 2012; 86 in 2013; 154 in 2014; 140 in 2015; 75 in first half of 2016), with diverse industrial and research applications using X-ray CT as means. This paper summarises the existence of the laboratory's first four years by way of selected examples, both from published and unpublished projects. In the process a detailed description of the capabilities and facilities available to users is presented.

© 2016 The Authors. Published by Elsevier B.V. This is an open access article under the CC BY license (<http://creativecommons.org/licenses/by/4.0/>).

1. Introduction

The history and principles of X-ray CT has a South African connection, as the physicist, Alan M. Cormack, who jointly developed the technique of computerised axial tomography (CAT) scanning with Godfrey N. Hounsfield, was born in South African [1]. More than 40 years later, South Africa is once more leading the way, leaving a relatively big footprint in X-ray CT applications, having a large number of systems installed across the country. In particular, three research institutions with accessible facilities: NECSA (The South African Nuclear Energy Corporation SOC Limited) that focus on research applications [2], Wits University focusing on fossils and paleontology, see e.g. [3] and the Stellenbosch University open access facility being described in this paper. The bi-annual national "Imaging with Radiation" conferences (most recently hosted in Stellenbosch [4]) bring together users from these various facilities and demonstrate the high quality applications-based research and development being done in South Africa with regards

to X-ray CT. Besides this presence, South Africa has been at the forefront of X-ray imaging development through the "full body Lodox scanner" developed locally [5] and originating from diamond scanners established at De Beers [6].

Principally, CAT or CT involves the acquisition of projection images from 360 degrees around the object, which are then reconstructed into a three-dimensional (3D) volume by using dedicated computer algorithms [7]. Since its first demonstration in 1971, CAT scanning found immediate use in the medical field, which lead to the Nobel Prize being awarded jointly to the developers of the technique, as mentioned above. Besides its huge impact in the medical field, the use of X-ray CT for investigating the internal details of objects non-destructively was also investigated from the early 1980's for non-medical applications. See, for example, some early work in materials science [8], wood science [9] and industrial applications [10]. This usage continuously increased as computing power, hardware and software advances were made, up to the point today where laboratory systems are available with resolutions up to 500 nm or better and voltages up to 450 kV or more. Software tools have become more user friendly and computer power has allowed ever larger volumes to be recorded and analysed.

* Corresponding author at: CT Scanner Facility, Central Analytical Facilities, Stellenbosch University, Stellenbosch, South Africa. Tel.: +27 21 808 9389.

E-mail addresses: anton2@sun.ac.za (A. du Plessis), lerouxsg@sun.ac.za (S.G. le Roux), aninag@sun.ac.za (A. Guelpa).

The diverse applications of modern X-ray CT is described in a number of recent reviews covering biology [11], food sciences [12], the geosciences [13], agricultural produce [14] as well as materials sciences [15,16], industrial applications [17] and metrology [18,19]. Non-destructive 3D imaging and analysis has emerged as a useful structural and dimensional analysis tool, starting to complement other more routine analytical tools i.e. scanning electron microscopy (SEM). In many cases X-ray CT offering unique insights, either by way of its non-destructive nature or its 3D imaging capability, revealing 3D structures not previously seen or understood. The driving force behind X-ray CT to become a more routine and accepted analytical technique (in the form of multi-user facilities such as the one described in this paper), is the ability to extract key parameters from images and then provide quantitative information. This paper aims to demonstrate the abilities and experience associated with the CT Scanner Facility at Stellenbosch University by showcasing a range of projects, both published and unpublished, from the first four years of its existence.

2. CT Scanner Facility

The CT Scanner Facility at Stellenbosch University houses a walk-in cabinet micro-CT scanner system for large samples, as well as a nano-CT scanner for highest resolution when using small samples, both manufactured by General Electric Sensing and Inspection Technologies/Phoenix X-ray (Wunstorff, Germany). The micro-CT scanner contains two X-ray tubes, one with a reflection-type target and the other with a transmission target, with the maximum voltage of the reflection target being 240 kV and that of the transmission target being 180 kV. Similarly, the nano-CT scanner is limited to 180 kV, though resolutions below 1 μm require less than 100 kV. The models are General Electric VTomex L240 and Nanotom S, and basic specifications are provided in Table 1.

The nanoCT instrument is well suited to small samples, and it is generally suggested that all samples (of any material type) smaller than 10 mm in diameter be scanned using the nanoCT instrument. The main reason for this is the better sample stability and the lower power X-ray tube which is very stable over long periods, ensuring sharper images from small samples. The transmission type X-ray tube has a diamond window fitted which results in increased X-ray emission compared to the typical transmission tube. This system also allows continuous scanning as an option, compared to typical stepwise rotation. This is useful for some applications where sample stability is an issue and allows relatively faster scans. Typical scan times are between 1 and 4 h for this system depending on resolution and quality requirements.

The microCT instrument is generally used for samples larger than 10 mm up to 300 mm in its longest axis. Larger samples are

possible but scan times become excessive and such samples are usually better suited to medical CT. Samples containing metal or rock are usually scanned preferably with the microCT instrument's high-power tube which allows up to 240 kV and high currents in reflection mode. This allows more beam filtration and a sharper image with less beam hardening and other artifacts. The microCT instrument also contains a transmission X-ray tube, similar to that in the nanoCT which is useful for large batches of smaller samples not requiring high power. It is also useful in the event of downtime of the high-power tube which occurs often for this type of system. Typical scan times for this system are between 30 min and 1.5 h depending on the resolution and quality requirements.

Voxel sizes mentioned above are calculated based on the geometrical magnification of the scan setup, i.e. The sample's distance from source and detector's distance from source. The voxel size and physical resolution are not necessarily the same, as the resolution can become very poor even with a good voxel size, when a very large X-ray spot is used, for example. However, under normal operating conditions the X-ray spot size is kept smaller than the voxel size and the distances of the sample and detector are kept such that the detector pixel size does not cause unsharpness. Therefore the terms voxel size and resolution are often interchangeably used. Systems are dimensionally calibrated in the factory and checked on a regular basis, as part of system maintenance. Additional dimensional calibrations can also be done as required.

Analysis can be performed on Windows (Microsoft Corporation, Washington, USA) workstations with multi-core CPUs, high-end graphics cards and between 64 and 128 GB random access memory (RAM). Most analysis tasks are performed with the software package Volume Graphics VGStudioMax 2.2 (Volume Graphics, Heidelberg, Germany) and the completed analysis, along with full volume data, is provided to the user with a corresponding free viewer program called myVGL (Volume Graphics, Heidelberg, Germany). Avizo Fire 9.0 (FEI, Oregon, USA) and Simpleware (Simpleware Ltd, Exeter, UK) software is also available at our facility's numerous workstations when users are required to do their own analysis, additionally having access to expert supervision and guidance when working at the facility.

As the CT Scanner Facility at Stellenbosch University is service orientated, analysis can also be performed on 3D data sets without the need for CT scanning, i.e. users who submit data via ftp file transfer. Other unique aspects related to this open access facility include very fast turnaround time due to high throughput requirements and the acceptance of all work, without any delays or application procedures. Furthermore, the user can be present or absent, depending on the requirement (that include sample loading, scanning, reconstruction, basic or advanced analysis, data transfer and return shipment or feedback session).

In the following section, special cases encountered at the CT Scanner Facility at Stellenbosch University are showcased. In these examples, the case study (objective) is stated, followed by highlighting valuable functionalities of CT scanning that allowed the respective study to be successful. This acts as a platform from where the capabilities of the CT Scanner Facility at Stellenbosch University is described, also reviewing the scientific outputs of the last four years (keeping in mind that some outputs might not have been disclosed, since the facility is open access).

3. Special cases encountered at the CT Scanner Facility at Stellenbosch University

3.1. Multi-scan process for long shaped samples

A study was conducted in order to investigate the porosity of the titanium casting process and to investigate the effect of hot iso-

Table 1
Basic specifications of the micro-CT and nano-CT systems at Stellenbosch University.

| | Direct tube | Nano focus tube | Nano-CT |
|--------------------------------------------------------------------------------------------------|-------------|-----------------|-------------|
| Voltage (kV) | 10–240 | 10–180 | 10–180 |
| Current (μA) | 5–3000 | 5–880 | 5–880 |
| Typical best voxel size (μm) | 5 | 2 | 0.5 |
| Beam angle ($^\circ$) | Approx. 30 | Approx. 180 | Approx. 180 |
| <i>Sample Limits (for single scan volume, multiple scans possible in X and Y with stitching)</i> | | | |
| Weight (kg) | 50 | 50 | 2 |
| Height (mm) | 320 | 320 | 150 |
| Width (mm) | 300 | 300 | 120 |
| <i>Typical maximum wall thickness of sample per material type, for best quality (mm)</i> | | | |
| Steel | 10 | | |
| Rock | 40 | | |
| Plastic | 100 | | |
| Wood | 200 | | |

static pressing (HIPping) on the porosity quantitatively [20]. As the rods were quite long (approx. 100 mm long and 30 mm wide), sections were scanned at high resolution and stitched together. As the best resolution limit (in μm) is roughly equal to the width of the sample in mm (a basic guideline), it was best to rather use multiple scans that would allow a higher resolution data set, compared to single scans of the elongated samples. This revealed some interesting and unexpected small sub-surface micro-porosity, at extremely low levels of average porosity (very few pores), which would have been almost impossible to detect by other means. This is also a good example of the same sample imaged before and after some processing step, in this case hot isostatic pressing (HIPping), which is meant to remove all porosity.

Another example of a long sample subjected to multi-scan, is one where a Ti6Al4V part produced by additive manufacturing was analysed at high resolution, before and after HIP treatment. The highest possible resolution revealed thin lack-of-fusion defects, which would have been impossible to detect by other means being, but ultimately a very important finding about the mechanical strength of the additive manufactured parts. It was also found that these defects were not sufficiently closed by HIP treatment, due to their connection to the surface [21].

3.2. Constructing density calibrations

One common misconception is that X-ray CT scans inherently produce density values in 3D. Although CT data can be calibrated for density determinations, as has been demonstrated by numerous authors, it is not a simple process. The reason being that scans need to be done with calibration standards in the same scan volume of the sample of interest. In our laboratory we have developed a unique method to calibrate densities for plastics and biological materials, as well as test whether the calibrations are accurate for the unknown materials by using a dual energy CT test [22]. The method works well for most biological samples and has been applied with great success to maize kernels [23]. It must be kept in mind that the voxel data is a grey value which can be recorded in various bit depths, also floating point format in some cases. In most cases in our laboratory we have standardized on using unsigned 16-bit data, which results in grey values between 0 and 65,535 (2^{16} for 16 bit data). These values vary according to the densest object in the scan volume, and therefore it is possible that metal and wood materials in two different subsequent scans can both have the same grey values of 50,000. But when the metal and wood are put together in a single scan, the metal may have a grey value of 50,000, while the wood will then have a much lower value e.g. 20,000. Furthermore, the wood can possibly have a similar density as the mounting material and even the surrounding air, making image processing very challenging.

It is important to realize that laboratory based X-ray sources are polychromatic in nature, which means that the grey values obtained (and attenuation coefficient) depends on the instrument (source, detector), its settings (kV, filtration), as well as the sample itself and the container or mounting material in the scan field of view.

3.3. More samples in one scan

The work of Guelpa et al. [23] was extended to demonstrate scanning of 150 maize kernels in one scan [24], thereby demonstrating the possibility of scanning many samples together to save time (and hence cost). Regardless the reduction in magnification (scanning 150 kernels at 100 μm rather than 10 μm for one kernel) sufficient detail was captured, along with the larger statistical analysis that could be performed in a shorter time (on features that are relatively large). However, this is only possible for very small

and low density samples. Usually the larger number of samples would reduce the penetration and thereby reduces the image quality along with the poorer resolution. Another successful application of this method was in work published from scans of bovine bone samples of 20 mm diameter [25,26].

Image quality in general is a difficult parameter to quantify: one method is to record grey values and their variance in the sample of interest and in the background, while another method is to record a line profile across the edge of a flat sample surface. In the first method, the signal to noise ratio shows the brightness of an image (and lack of noise), while the line profile will show edge sharpness. Image quality depends on various parameters but when considering polychromatic laboratory based X-ray sources and typical samples, the grey value variations are much larger than the bin size even in 8-bit data types. Since the detectors used are typically from 12 to 16 bit in depth, any further data depth will not result in improved image quality. In fact even 8-bit would be sufficient in most cases without a significant lack of image quality.

3.4. Imaging cellular structure

Since the Stellenbosch CT facility is housed in the Department of Forestry and Wood Science, numerous wood science projects have been conducted. These include the investigation of wood cellular structure degradation due to fire damage [27] and the observation of cell-wall density changes in welded beech wood [28], amongst others. Both these studies involved high resolution scans of small sections of wood and the interest was in visualising and quantifying the cell wall densities. Cutting such samples damage the cell walls, thereby making X-ray CT a preferred analysis method compared to surface analysis tools. In these case studies the samples were between 0.5 and 2.5 mm in diameter, with voxel sizes ranging from 0.5 to 2 μm . Wood cells have thicknesses in the range of 2–8 μm , therefore their imaging is relatively simple by micro-CT and nano-CT. High quality 3D images of cellular structures such as wood allow simulations to be performed to investigate material dynamic properties such as permeability, which can be useful for understanding physical structures that hamper or enhance flow rates, and for comparing different types of samples with regards to permeability. In Fig. 1 a simulation is shown on a Eucalyptus wood sample of 500 μm width. The outputs from a simulation include absolute permeability and flow rate values.

3.5. Geological and paleontological applications

In terms of geological applications, one recent example was the analysis of exploration drill cores containing tungsten minerals and the quantification of the total volumetric tungsten mineral content thereof [29]. Conventionally, the standard industry technique of crushing along with chemical analysis is followed, but the X-ray CT method was very accurate compared to the traditional method and much faster, even providing additional information on particle sizes. Other geological applications include analysis of microwave-treated ore particles during a long-term heap leaching experiment [30,31] where the development of cracks and removal of minerals could be directly visualised in the same particles subjected to time-lapse X-rayCT experiments. A recently published result from our facility highlighted the 3D and directionality information that can assist in understanding deposition mechanisms of mineral deposits, i.e. barite in a paleosol environment in this particular case [32]. Further work has also been conducted on the visualisation of diamonds in situ in kimberlite rocks [33] and also in cut diamonds for fingerprinting of individual stones by their unique inclusions (their 3D locations) [34,35].

Paleontology and archeology are fields which have embraced the use of X-ray CT for non-destructive analysis of fossils, some-

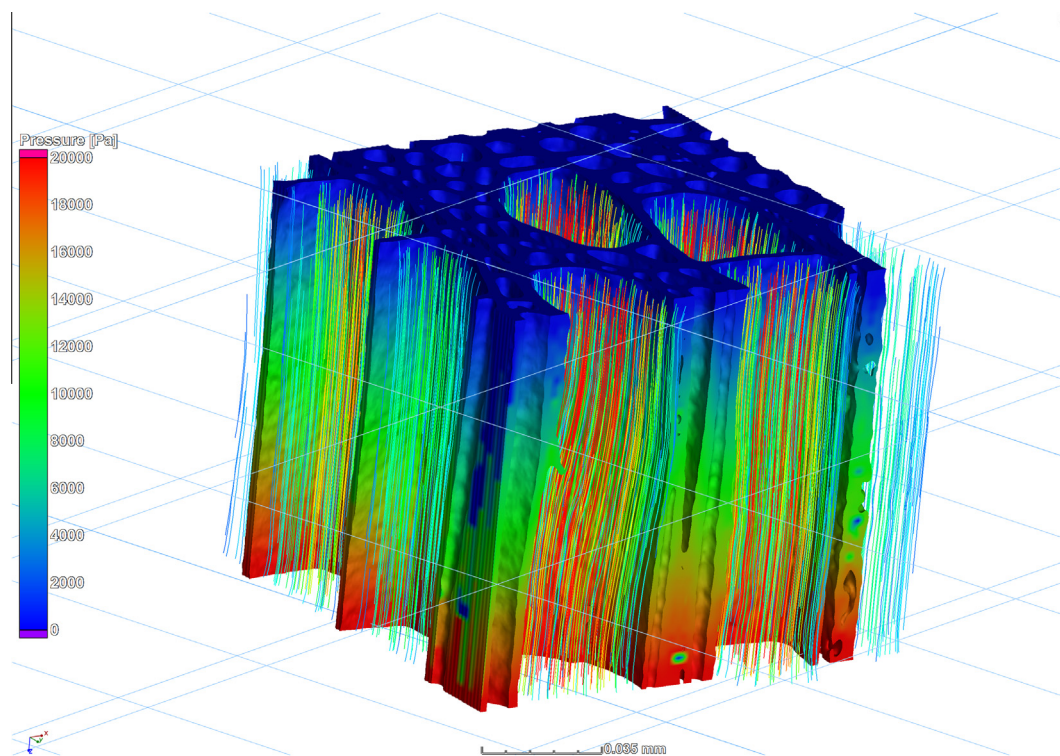


Fig. 1. Imaging cellular structure in 3D allows image-based simulations, e.g. of fluid flow. Visualised here is the cellular structure of a selected cube of eucalyptus wood of 500 μm wide, to which a simple fluid flow simulation was applied using the viscosity of water and a pressure difference as input parameters. The absolute permeability is determined, which is close to the literature values known from this wood type.

times still embedded inside host rock. One example from our laboratory is provided in [36], where it was shown that the X-ray CT data could be used as a starting point for laser processing (to remove rock by laser ablation according to the 3D data). Another recent example is that of a frog species and comparison of bone morphology of modern frogs to that of fossils of extinct frogs, using advanced image processing techniques [37].

3.6. Ancient artifacts

Ancient artifacts, such as Egyptian mummies, are well suited to non-destructive analysis by X-ray CT. One good example is that of animal mummies hosted in South African museums, which were subjected to micro-CT scans. Many of these were found to be fakes (containing only reeds or parts of animals), while others were actual well preserved full animals [38]. The data of one of the fully preserved animals was used to create a CAD file and subsequently 3D printed, which was aimed at increasing the impact of the museum display [39]. One of the samples was found to contain interesting and unexpected stomach contents after being analysed by a high resolution close-up scan. Even though the outside of the sample entirely filled the field of view of the detector, this close-up (volume-of-interest or a sub-volume) scan was possible. The higher resolution allowed strikingly clear visualisation of a mass of bones as seen in Fig. 2, and upon closer inspection, it was found to be the remains of a number of different rodents and a small bird, indicating over-feeding and subsequent early falconry in ancient Egypt [40].

3.7. Biological applications

Biological applications can be quite remarkable and one excellent example from our facility is that of brooding brittle stars (with babies inside in their natural state) [41,42], which would not have

been possible to view in any other imaging modality. One striking image is shown in Fig. 3, where the combination of high and low resolution scans allows the imaging of the internal details, as well as the exterior in full, including the legs of the brittle star.

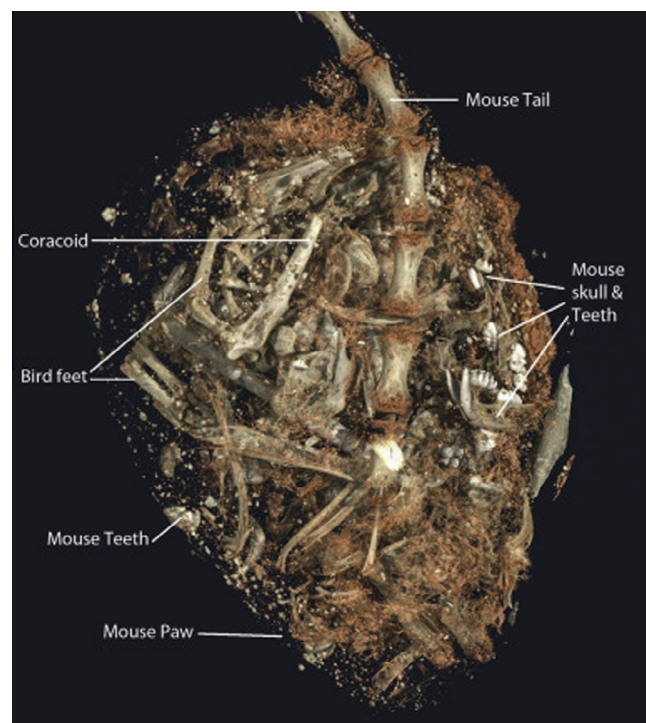


Fig. 2. Stomach contents of an animal mummy preserved for approximately 2000 years and analysed non-destructively by high resolution X-ray CT, revealing remains of mice and a small bird (reproduced with permission from [40]).

3.8. Additive manufacturing

Additive manufacturing and 3D printing has been of particular interest in our facility, as already demonstrated in a 2012 conference paper [43] and subsequently, a series of studies were completed on: the quantification of print quality from consumer printers [44], directionality found in porosity of such parts [45], lack of fusion defects which could be identified before and after HIP treatment [21] and, more recently, some work on quality control of medical implants produced by additive manufacturing [46] and the analysis of Ti6Al4V tensile samples before and after loading [47]. Besides these efforts, the Stellenbosch Idea2Product lab [48] was initiated in 2015 and continues to print objects on-demand, also from X-ray CT data.

3.9. Facilitating large numbers of samples

One of the useful aspects of an open access facility is the larger number of samples that can be analysed cost effectively, allowing statistically effective sample numbers. Usually, a particular analysis is first optimised in terms of scan quality and type, as well as analysis requirements, following a decision on batch size. Performing scans and analyses in batches (on large numbers of samples) also assists in keeping the quality between scans directly comparable. Some of the largest numbers of samples scanned to date are lizards, pears and plums. The large series of lizards scans (approximately 400 lizards) were scanned recently and this work is still being processed and will be published in the near future. The pears and plums were the topics of two different horticultural studies over the last 4 years [49–51]. The total number of pears scanned exceeds 200, at 30–60 min scan time per pear. Plums were approximately 100 at specific times of development, at 30–40 min scan time per plum.

3.10. Industrial applications

Industrial applications are seldom reported, but we have described one example illustrating the type of analysis possible for “routine” X-ray CT analysis [52], while another conference paper demonstrates the ability to test an airplane engine casing [53]. Instead of reporting any industrial work, an example is shown in Fig. 4 of an Image Quality Indicator (IQI) which is typically used in industrial X-ray inspection using 2D X-ray images. In this case, we scanned this object and found the thickness values to be slightly different than specified, due to the wires not being perfectly cylindrical. The IQI (DIN62FE, 10ISO16) has specified diameters of 0.40 mm, 0.32 mm, 0.25 mm, 0.20 mm, 0.16 mm, 0.13 mm and 0.10 mm, respectively. It is worth mentioning that for high quality scans, sub-voxel accuracy is possible, which means that dimensional accuracy is guaranteed to be better than the voxel size of the scan. A full description of this sub-voxel precision is not relevant here, but some information can be found in [54] and the ASTM standard for ensuring high scan quality can be found in [55].

In this particular case, the scan data was analysed using the advanced surface determination function in VGStudioMax 2.2, followed by best-fit cylinders fitted to the central section of each wire and diameters measured as shown in Fig. 4. These diameter values are very close to the expected values, except for the smallest one which is visually seen to be non-cylindrical in the CT slice data. The CT cross-sectional slice images for the largest and smallest wires are available as [supplementary material](#). This scan was done with a 25 μm voxel size, allowing 4 voxels across the thinnest wire of 100 μm wire. When considering grey value differences, the error in segmentation of the edge of a material can be understood as being as much as one or two voxels on either side of the wire, taking this case as example. With the help of sub-voxel interpolation of grey values and advanced algorithms incorporating local optimization in addition to global thresholding, the edge determination can

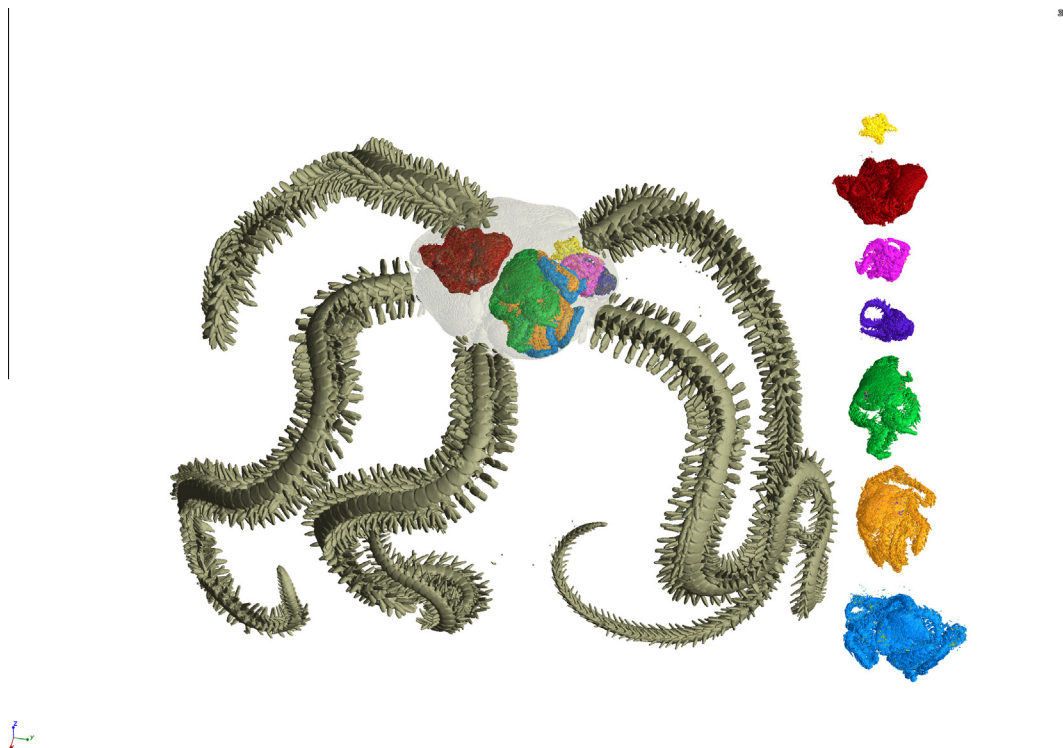


Fig. 3. A brittle star with 7 babies segmented by colour. This image was taken through a combination of low and high resolution scans, merging the scans and manual segmentation of the young. Image courtesy of Jannes Landschoff.

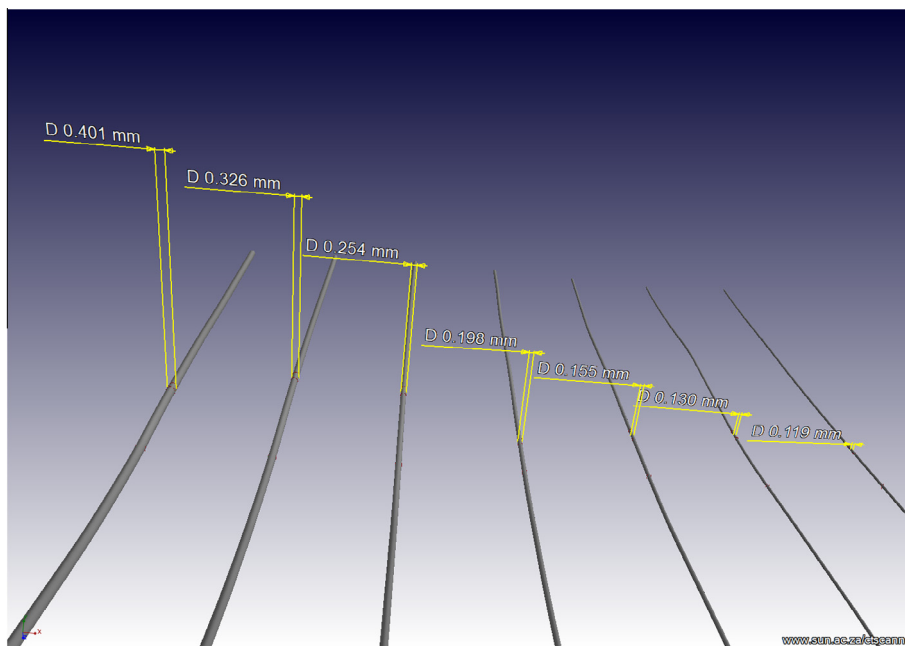


Fig. 4. IQI wires and CT measurement of their cylindrical thickness values using metrology tools in the 3D analysis software. Additional images available as [supplementary material](#).

be more accurate than the voxel size. The accuracy and precision are strongly influenced by the data quality, and the dimensional calibration of the CT system.

3.11. Other applications

A variety of engineering applications with a research focus have been completed successfully. From civil engineering examples of interest were in quantifying porosity in high performance concretes [56,57], pore networks in collapsible soils [58], as well as metal reinforcement in concrete and its distribution (not published). Some work in mechanical engineering has been reported [59,60]. A particularly successful project involved high resolution imaging of fuel cell components and assisted in understanding the structural details such as layer thickness, coating thickness and the merging of coatings into fiber materials [61,62].

Food sciences and applied agricultural sciences has been a significant user of our facility as is demonstrated by a review article of X-ray CT in food sciences [12]. Some student projects with respect to maize kernel analysis have been completed [63,64], along with associated publications reporting on maize kernel endosperm volumes and their relation to hardness, density calibrations and determination of 3D density of maize kernels [23] and a high-throughput methodology for this process [24]. Some work regarding processing of wheat and comparing the oven and forced convection methods, have been reported in [65] and ongoing work in wheat, maize, popcorn and applications of food sciences and 3D imaging are in process. Horticultural work reported include pomegranate analysis [66,67], pears and plums as mentioned in the section on large sample sets [49–51].

3.12. Strange samples

Some of the strangest samples scanned are briefly described here. One particularly strange example was that of roots of vine plants containing live bugs, scanned in order to visualise the location and extend of bug infestation “in situ”. The bugs moved around during the scan, sometimes causing a blur, which necessitated fast

scanning to minimise the blur. Another strange request was that of small (<1 mm diameter) spherical shaped bones from the inside of fish ears, for morphological analysis. This sample type can easily be misplaced and sample mounting is challenging. Finally, a “fresh dead” guinea fowl, still undergoing rigor mortis, was scanned to determine the location and extend of pellets in the meat, from the shotgun used. The challenge was to load the guinea fowl in a bucket with tape to keep it in place for the scan, even while rigor mortis was setting in which caused movement. Other relatively strange samples include a silkworm larva where its tracheal system was imaged [68], a shrimp, leaves with hairs, sweet potato powders and chicken bones.

4. Conclusion

The aim here was to demonstrate the varied applications of X-ray CT in the Stellenbosch University multi-user facility and through these examples show how X-ray CT can be used for different types of non-destructive investigations. A recent paper also compares medical and microCT for the purpose of typical non-destructive testing, which shows the benefits and limitations of both techniques [69]. Further examples can be found at the regularly updated website of the facility (<http://www.sun.ac.za/ctscanner>) as well as its regular newsletters also found on the website. The first four years have seen significant growth and we envisage the applications to continue to be as diverse, and we hope that the open access nature will lead to many discoveries not previously possible.

Acknowledgements

We would like to acknowledge the National Research Foundation's National Equipment Program for funding the micro-CT and nano-CT instruments through grants UID72325 and UID88057. The National Research Foundation also supports our facility through the Internship program, placing intern students in our facility for 12 month periods (total of 9 so far placed, 8 completed). Since our facility is of open-access format, we acknowledge the

loyal support of all users of our facility, as the combined usage is what financially supports our facility (besides equipment cost and office space). We also would like to acknowledge the main applicants for the equipment grants mentioned above, Prof Thomas Seifert and Prof Marena Manley, for their contributions to this facility.

Appendix A. Supplementary data

Supplementary data associated with this article can be found, in the online version, at <http://dx.doi.org/10.1016/j.nimb.2016.08.005>.

References

- [1] A. Cormack, Reconstruction of densities from their projections, with applications in radiological physics, *Phys. Med. Biol.* 18 (1973) 195.
- [2] F. De Beer, Characteristics of the neutron/X-ray tomography system at the SANRAD facility in South Africa, *Nucl. Instrum. Methods Phys. Res. Sect. A* 542 (2005) 1–8.
- [3] J.A. Ledogar, A.L. Smith, S. Benazzi, G.W. Weber, M.A. Spencer, K.B. Carlson, K.P. McNulty, P.C. Dechow, I.R. Grosse, C.F. Ross, Mechanical evidence that *Australopithecus sediba* was limited in its ability to eat hard foods, *Nat. Commun.* 7 (2016).
- [4] <<http://blogs.sun.ac.za/ctscanner/files/2015/02/IMG2015-PROGRAM.pdf>>. (accessed 16.06.16).
- [5] S. Beningfield, H. Potgieter, A. Nicol, S. Van As, G. Bowie, E. Hering, E. Lätti, Report on a new type of trauma full-body digital X-ray machine, *Emerg. Radiol.* 10 (2003) 23–29.
- [6] J. Danoczi, A. Koursaris, Development of luminescent diamond simulants for X-ray recovery, *J. South Afr. Inst. Min. Metall.* 108 (2008) 89–97.
- [7] A.C. Kak, M. Slaney, Principles of Computerized Tomographic Imaging, IEEE Press, New York, 1988, pp. 104–107.
- [8] J. Kinney, Q. Johnson, U. Bonse, M. Nichols, R. Saroyan, R. Nusshardt, R. Pahl, J. Brase, Three dimensional X-ray computed tomography in materials science, *MRS Bull.* 13 (1988) 13–18.
- [9] M. Onoe, J.W. Tsao, H. Yamada, H. Nakamura, J. Kogure, H. Kawamura, M. Yoshimatsu, Computed tomography for measuring the annual rings of a live tree, *Nucl. Instrum. Methods Phys. Res.* 221 (1984) 213–220.
- [10] W. Gilboy, X-and γ -ray tomography in NDE applications, *Nucl. Instrum. Methods Phys. Res.* 221 (1984) 193–200.
- [11] R. Mizutani, Y. Suzuki, X-ray microtomography in biology, *Micron* 43 (2012) 104–115.
- [12] L. Schoeman, P. Williams, A. du Plessis, M. Manley, X-ray micro-computed tomography (μ CT) for non-destructive characterisation of food microstructure, *Trends Food Sci. Technol.* 47 (2016) 10–24.
- [13] V. Cnudde, M.N. Boone, High-resolution X-ray computed tomography in geosciences: a review of the current technology and applications, *Earth Sci. Rev.* 123 (2013) 1–17.
- [14] N. Kotwaliwale, K. Singh, A. Kalne, S.N. Jha, N. Seth, A. Kar, X-ray imaging methods for internal quality evaluation of agricultural produce, *J. Food Sci. Technol.* 51 (2011) 1–15.
- [15] E. Maire, P.J. Withers, Quantitative X-ray tomography, *Int. Mater. Rev.* 59 (2014) 1–43.
- [16] E.N. Landis, D.T. Keane, X-ray microtomography, *Mater. Charact.* 61 (2010) 1305–1316.
- [17] L. De Chiffre, S. Carmignato, J.-P. Kruth, R. Schmitt, A. Weckenmann, Industrial Applications of Computed Tomography, *CIRP Ann. Manuf. Technol.* 63 (2014) 655–677.
- [18] J.P. Kruth, M. Bartscher, S. Carmignato, R. Schmitt, L. De Chiffre, A. Weckenmann, Computed tomography for dimensional metrology, *CIRP Ann. Manuf. Technol.* 60 (2011) 821–842.
- [19] F. Léonard, S. Brown, P. Withers, P. Mummery, M. McCarthy, A new method of performance verification for X-ray computed tomography measurements, *Meas. Sci. Technol.* 25 (2014) 065401.
- [20] A. du Plessis, P. Rossouw, Investigation of porosity changes in cast Ti6Al4V rods after hot isostatic pressing, *J. Mater. Eng. Perform.* 24 (2015) 3137–3141.
- [21] A. du Plessis, S.G. le Roux, J. Els, G. Booyens, D.C. Blaine, Application of microCT to the non-destructive testing of an additive manufactured titanium component, *Case Stud. Nondestruct. Test. Eval.* 4 (2015) 1–7.
- [22] A. Du Plessis, M. Meincken, T. Seifert, Quantitative determination of density and mass of polymeric materials using microfocus computed tomography, *J. Nondestruct. Eval.* 32 (2013) 413–417.
- [23] A. Guelpa, A. Du Plessis, M. Kidd, M. Manley, Non-destructive estimation of maize (*Zea mays* L.) Kernel hardness by means of an X-ray micro-computed tomography (μ CT) density calibration, *Food Bioprocess Technol.* 8 (2015) 1419–1429.
- [24] A. Guelpa, A. du Plessis, M. Manley, A high-throughput X-ray micro-computed tomography (μ CT) approach for measuring single kernel maize (*Zea mays* L.) volumes and densities, *J. Cereal Sci.* 69 (2016) 321–328.
- [25] G. Dubois, M. Prot, S. Laporte, T. Cloete, What is the recommended size of a Volume of Interest for cancellous bone? A skeleton-based study, *Comput. Methods Biomech. Biomed. Eng.* 18 (2015) 1932–1933.
- [26] M. Prot, G. Dubois, T. Cloete, D. Saletti, S. Laporte, Fracture characterization in cancellous bone specimens via surface difference evaluation of 3D registered pre-and post-compression micro-CT scans, *Comput. Methods Biomech. Biomed. Eng.* 18 (2015) 2030–2031.
- [27] M. Meincken, A. du Plessis, Visualising and quantifying thermal degradation of wood by computed tomography, *Eur. J. Wood Wood Prod.* 71 (2013) 387–389.
- [28] M. Vaziri, A.D. Plessis, D. Sandberg, S. Berg, Nano X-ray tomography analysis of the cell-wall density of welded beech joints, *Wood Mat. Sci. Eng.* 10 (2015) 368–372.
- [29] S.G. Le Roux, A. Du Plessis, A. Rozendaal, The quantitative analysis of tungsten ore using X-ray microCT: case study, *Comput. Geosci.* 85 (2015) 75–80.
- [30] E. Charikinya, S. Bradshaw, A. du Plessis, X-ray computed tomography visualisation and quantification of microwave induced cracks in particles.
- [31] E. Charikinya, Characterising the Effect of Microwave Treatment on Bio-Leaching of Coarse, Massive Sulphide Ore Particles (Thesis), Stellenbosch University, Stellenbosch, 2015.
- [32] C.E. Clarke, T.O. Majodina, A. du Plessis, M.A.G. Andreoli, The use of X-ray tomography in defining the spatial distribution of barite in the fluvially derived palaeosols of Vaalputs, Northern Cape Province, South Africa, *Geoderma* 267 (2016) 48–57.
- [33] S. Richardson, R. Kahle, B. Shaw-Kahle, J. Gurney, A. du Plessis, Metasomatic Diamond Formation revealed by X-Ray CT Scanning of Diamondiferous Eclogites from Southern Africa, AGU Fall Meeting Abstracts, 2014, pp. 5.
- [34] J. Roux, Classification of Diamonds by Microfocus X-Ray Computed Tomography (Thesis), Department of Earth Sciences, University of Stellenbosch, 2012.
- [35] A. du Plessis, J.S.G. Roux, A. Rozendaal, A. Tolken, Characterization of cut diamonds by X-ray tomography, *Gems Gemol.* (2016) (in review).
- [36] A. du Plessis, J. Steyn, D.E. Roberts, L.R. Botha, L.R. Berger, A proof of concept demonstration of the automated laser removal of rock from a fossil using 3D X-ray tomography data, *J. Archaeol. Sci.* 40 (2013) 4607–4611.
- [37] T. Matthews, A. du Plessis, Using X-ray computed tomography analysis tools to compare the skeletal element morphology of fossil and modern frog (*Anura*) species, *Palaeontol. Electronica* 19 (2016) 1–46.
- [38] I. Cornelius, L. Swanepoel, A. Du Plessis, R. Slabbert, Looking inside votive creatures: Computed tomography (CT) scanning of ancient Egyptian mummified animals in Iziko Museums of South Africa: a preliminary report, *Akroterion* 57 (2012) 129–148.
- [39] A. Du Plessis, R. Slabbert, L.C. Swanepoel, J. Els, G.J. Booyens, S. Ikram, I. Cornelius, Three-dimensional model of an ancient Egyptian falcon mummy skeleton, *Rapid Prototyping J.* 21 (2015) 368–372.
- [40] S. Ikram, R. Slabbert, I. Cornelius, A. du Plessis, L.C. Swanepoel, H. Weber, Fatal force-feeding or Gluttonous Gagging? The death of Kestrel SACHM 2575, *J. Archaeol. Sci.* 63 (2015) 72–77.
- [41] J. Landschoff, A. Du Plessis, C.L. Griffiths, A dataset describing brooding in three species of South African brittle stars, comprising seven high-resolution, micro X-ray computed tomography scans, *GigaScience* 4 (2015) 1–4.
- [42] J. Landschoff, C. Griffiths, Three-dimensional visualisation of brooding behaviour in two distantly related brittle stars from South African waters, *Afr. J. Mar. Sci.* 37 (2015) 533–541.
- [43] A. Du Plessis, T. Seifert, G. Booyens, J. Els, Microfocus X-ray computed tomography (CT) analysis of laser sintered parts, *S. Afr. J. Ind. Eng.* 25 (2014) 39–49.
- [44] A. du Plessis, S.G. le Roux, F. Steyn, X-ray computed tomography of consumer-grade 3D-printed parts, *3D Print. Addit. Manuf.* 2 (2015) 190–195.
- [45] A. du Plessis, S.G. le Roux, G. Booyens, J. Els, Directionality of cavities and porosity formation in powder-bed laser additive manufacturing of metal components investigated using X-ray tomography, *3D Print. Addit. Manuf.* 3 (2016) 48–55.
- [46] A. Du Plessis, G. Booyens, J. Els, Quality control of a laser additive manufactured medical implant by X-ray tomography, *3D Print. Addit. Manuf.* (2016) (in press).
- [47] F.G. Krakhmalev, P. I. Yadroitsava, N. Kazantseva, A. du Plessis, I. Yadroitsev, Deformation behavior and microstructure of Ti6Al4V manufactured by SLM, *Phys. Procedia* (2016) (in review).
- [48] <<http://blogs.sun.ac.za/idea2product/>>. (accessed 16.06.16).
- [49] T. Muziri, The influence of cell wall bound calcium, cell number and size on the development of mealiness in “forelle” pear. Evaluation of X-ray CT and NIR as non-destructive techniques for mealiness detection (Thesis), University of Stellenbosch, 2016.
- [50] T. Muziri, K. Theron, E. Crouch, Mealiness development in “Forele” pears (*Pyrus communis* L.) is influenced by cell size, in: XII International Pear Symposium, vol. 1094, 2014, pp. 515–523.
- [51] I. Kritzinger, A Study of Broken Stones in Japanese Plums (*Prunus salicina* Lindl.) (Thesis), Stellenbosch University, Stellenbosch, 2015.
- [52] A. du Plessis, P. Rossouw, X-ray computed tomography of a titanium aerospace investment casting, *Case Stud. Nondestruct. Test. Eval.* 3 (2015) 21–26.
- [53] A. du Plessis, S.G. le Roux, H. van Rooyen, 3D X-ray inspection of a radio controlled airplane engine, *Mater. Sci. Forum* 828–829 (2015) 433–438. 6p.
- [54] H. Villarraga, E. Morse, R. Hocken, S. Smith, Dimensional metrology of internal features with x-ray computed tomography, in: Proceedings of ASPE Annual Meeting, 2014.

- [55] ASTM E1570-11, Standard Practice for Computed Tomographic (CT) Examination, ASTM International, West Conshohocken, PA, 2011. <www.astm.org>.
- [56] A. du Plessis, B.J. Olawuyi, W.P. Boshoff, S.G. le Roux, Simple and fast porosity analysis of concrete using X-ray computed tomography, *Mater. Struct.* 49 (2016) 553–562.
- [57] B.J. Olawuyi, The Mechanical Behaviour of High-Performance Concrete with Superabsorbent Polymers (SAP) (Thesis), Stellenbosch University, Stellenbosch, 2016.
- [58] S.Y. Asante, Alternate methods to determine the microstructure of collapsible soils (Thesis), Stellenbosch University, Stellenbosch, 2015.
- [59] T. Becker, M. van Rooyen, D. Dimitrov, Heat treatment of Ti-6Al-4V produced by laser cutting, *S. Afr. J. Ind. Eng.* 26 (2015) 93–103.
- [60] T.H. Becker, M. Beck, C. Scheffer, Microstructure and mechanical properties of direct metal laser sintered Ti-6Al-4V, *S. Afr. J. Ind. Eng.* 26 (2015) 1–10.
- [61] O.S. Burheim, G.A. Crymble, R. Bock, N. Hussain, S. Pasupathi, A. du Plessis, S. le Roux, F. Seland, H. Su, B.G. Pollet, Thermal conductivity in the three layered regions of micro porous layer coated porous transport layers for the PEM fuel cell, *Int. J. Hydrogen Energy* 40 (2015) 16775–16785.
- [62] G.A. Crymble, Towards Reliable Correlation of Microporous Layer Physical Characteristics and PEMFC Electrochemical Performance (Thesis), Stellenbosch University, Stellenbosch, 2014.
- [63] T. Mokhorro, Investigating the impact of pre-harvesting sprouting on maize hardness using near infrared (NIR) hyperspectral imaging and X-ray micro-computed tomography (μ CT) (Thesis), Stellenbosch University, 2016.
- [64] A. Guelpa, Maize Endosperm Texture Characterisation Using the Rapid Visco Analyser (RVA), X-Ray Micro-Computed Tomography (μ CT) and Micro-Near Infrared (microNIR) Spectroscopy (Thesis), Stellenbosch University, Stellenbosch, 2015.
- [65] L. Schoeman, A. du Plessis, M. Manley, Non-destructive characterisation and quantification of the effect of conventional oven and forced convection continuous tumble (FCCT) roasting on the three-dimensional microstructure of whole wheat kernels using X-ray micro-computed tomography (μ CT), *J. Food Eng.* 187 (2016) 1–13.
- [66] L.S. Magwaza, U.L. Opara, Investigating non-destructive quantification and characterization of pomegranate fruit internal structure using X-ray computed tomography, *Postharvest Biol. Technol.* 95 (2014) 1–6.
- [67] E. Arendse, O.A. Fawole, L.S. Magwaza, U.L. Opara, Non-destructive characterization and volume estimation of pomegranate fruit external and internal morphological fractions using X-ray computed tomography, *J. Food Eng.* 186 (2016) 42–49.
- [68] P.G. Matthews, J.S. Terblanche, Chapter one-evolution of the mechanisms underlying insect respiratory gas exchange, *Adv. Insect Physiol.* 49 (2015) 1–24.
- [69] A. du Plessis, S.G. le Roux, A. Guelpa, Comparison of medical and industrial X-ray computed tomography for non-destructive testing, *Case Stud. Nondestruct. Test. Eval.* 6 (2016) 17–25.